Effect of structural disorder on quantum oscillations in graphite

B. C. Camargo, Y. Kopelevich, A. Usher, and S. B. Hubbard

Citation: Applied Physics Letters **108**, 031604 (2016); doi: 10.1063/1.4940233

View online: http://dx.doi.org/10.1063/1.4940233

View Table of Contents: http://scitation.aip.org/content/aip/journal/apl/108/3?ver=pdfcov

Published by the AIP Publishing

Effect of structural disorder on quantum oscillations in graphite

B. C. Camargo,[1,a)] Y. Kopelevich,[1] A. Usher,[2] and S. B. Hubbard[2]
[1]*Instituto de Fisica Gleb Wataghin, Universidade Estadual de Campinas, Unicamp 13083-970, Campinas, São Paulo, Brazil*
[2]*School of Physics, University of Exeter, Stocker Road, Exeter EX4 4QL, United Kingdom*

(Received 21 October 2015; accepted 8 January 2016; published online 21 January 2016)

We have studied the effect of structural disorder on the de Haas van Alphen and Shubnikov de Haas quantum oscillations measured in natural, Kish, and highly oriented pyrolytic graphite samples at temperatures down to 30 mK and at magnetic fields up to 14 T. The measurements were performed on different samples characterized by means of x-ray diffractometry, transmission electron microscopy, and atomic-force microscopy techniques. Our results reveal a correlation between the amplitude of quantum oscillations and the sample surface roughness. © *2016 AIP Publishing LLC*.
[http://dx.doi.org/10.1063/1.4940233]

Graphite is one of the allotrope forms of carbon consisting of weakly bonded layers of graphene. Research in the past decade has shown that graphite exhibits some of the properties of graphene, most notably the presence of Dirac fermions,[1,2] along with other remarkable properties, such as the occurrence of the quantum Hall effect (QHE), ferromagnetism, and magnetic-field-driven metal insulator transitions.[3–5]

At low temperatures, highly oriented graphite presents clear quantum oscillations in its magnetic susceptibility and electric resistivity. It is known that these oscillatory phenomena (namely, the de Haas van Alphen (dHvA) and Shubnikov de Haas (SdH) effects) are suppressed by sample disorder. Textbook results show that the amplitude ΔM of these effects relate mainly to the width Γ of the Landau levels, which is affected by the effective mass of charge carriers and electronic scattering rates[3,6]

$$\Delta M \propto \frac{\lambda}{\sinh\lambda}\exp\left(-2\pi\frac{\Gamma}{\hbar\omega_c}\right), \tag{1}$$

where ω_c the cyclotronic frequency of the carriers and $\lambda = 2\pi^2 k_B T/\hbar\omega_c$. These parameters do not trivially relate to structural disorder of samples, as some structural faults might enhance electronic transport instead of hindering it (e.g., heterojunctions or tensile strains are responsible for high-mobility electron gases in semiconducting systems).[7,8]

In graphite, the parameter usually held as a measurement of sample quality is its mosaic spread (see, for example, Refs. 9 and 10). However, other disorder parameters can be equally important in characterizing sample quality, while not directly related to its mosaicity. For example, line-like defects and grain boundaries in highly oriented pyrolytic graphite (HOPG) can harbor ferromagnetic domains and strongly affect the samples' electric transport properties.[9,11,12] In addition, reduced crystallite sizes in graphite are known to impair the material electronic mobility and increase the ratio between the G and D peaks observed in Raman spectroscopy measurements.[13] Furthermore, small-angle rotational stacking faults in HOPG have been shown to cause interfaces between graphitic regions inside macroscopic samples, which are proposed to hold exotic states.[14]

In particular, no study identifying the structural disorder parameters responsible for the suppression of quantum oscillations in graphite has been reported to date. For this reason, in this work, we correlate the parameters of the dHvA and SdH effects in different types of HOPG with their structural properties. Our results strongly suggest that irregularities caused by corrugations (here called surface roughness) are the fundamental disorder parameter affecting quantum oscillations in graphite.

Our samples were five different grades of HOPG from SPI-Supplies[10] (designated SPI-I; SPI-II; SPI-III; GW; and ZYB), Kish,[15] and natural graphite. They were characterized by x-ray diffractometry, magnetotransport, and magnetic susceptibility measurements. Magnetotransport experiments were performed using a standard 4-probe measurement technique. Magnetization measurements were performed in a commercial Quantum Design SQUID (Superconducting Quantum Interference Device) magnetometer[16] and using the torsion-balance magnetometer described in Ref. 17. Experiments were carried out in the temperature range $2\,\mathrm{K} < T < 4\,\mathrm{K}$ for the SQUID (which used a conventional He-4 flow cryostat) and at $30\,\mathrm{mK} < T < 2\,\mathrm{K}$ for the torque magnetometer (which used a He-3 dilution fridge). Measurements in the SQUID setup were performed in DC mode. Experiments with the torque magnetometer were conducted by measuring the displacement of a balanced rotor via capacitive proximity detection with a pre-calibrated capacitor bridge.[17] Both systems were equipped with superconducting coils, allowing for measurements in the magnetic field range $-14\,\mathrm{T} < B < 14\,\mathrm{T}$ (torque) and $-7\,\mathrm{T} < B < 7\,\mathrm{T}$ (SQUID). The magnetic field was applied parallel to the sample c-axis in the case of the magnetotransport and SQUID experiments, and at 20° with respect to the c-axis in the case of the torsion-balance experiments.

Initially, all samples were characterized by means of x-ray diffractometry. Figure 1 shows the rocking-curves measured around the [0001] peak of graphite ($2\theta = 26°$). Samples GW, ZYB, Kish, and natural graphite presented curves with several peaks and will be labeled "group M". Samples SPI-I, SPI-II, and SPI-III showed a single peak

a)Electronic mail: b.c_camargo@yahoo.com.br

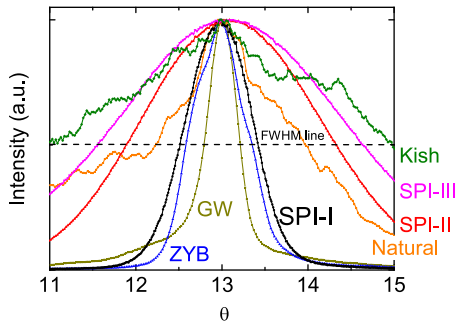

FIG. 1. Rocking curves of the samples studied. The dashed line represents where the FWHM is measured. All curves were normalized to the unity.

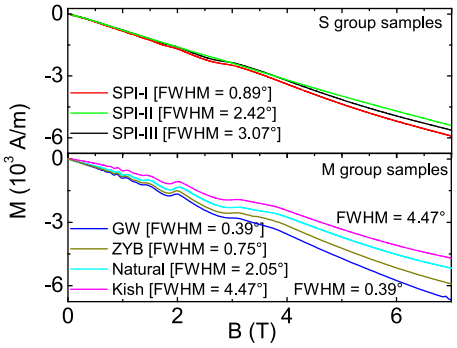

FIG. 2. Magnetic moment vs magnetic field measured in a SQUID magnetometer at $T = 2\,\mathrm{K}$ for different HOPG grades. The upper (lower) panel shows the curves for S (M) samples.

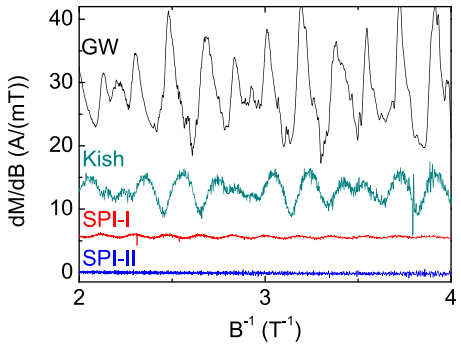

FIG. 3. dHvA oscillations for four different types of graphite. All measurements were carried out on a torque magnetometer at 30 mK. Successive curves are offset vertically for clarity.

behavior and will be called "group S." The multiple peak behavior in the M group suggests that these samples are composed by large, slightly misaligned, flat blocks of HOPG. The full-widths at half-maximum (FWHM) for each curve were extracted as shown in the figure. They are listed in Table I and are considered the samples' mosaicity.

Field-dependent magnetization (M(B) measurements at $T = 2\,\mathrm{K}$ showed the presence of the dHvA effect in all samples, except in SPI-II. The data, presented in Figure 2, show that S samples have weaker quantum oscillations than M samples, regardless of their values of FWHM. This result suggests that the sample mosaicity cannot be held accountable for the amplitude of the quantum oscillations measured. For example, the samples Kish ($FWHM = 4.47°$) and natural graphite ($FWHM = 2.05°$) present stronger dHvA effect than all SPI samples (max. $FWHM = 3.07°$), while having a wider mosaic spread. This difference is more evident at lower temperatures, as shown in Fig. 3.

We further note that S samples presented dHvA oscillations with a single frequency component, in opposition to the two frequencies found in M samples. Although SPI-II had no dHvA oscillations down to 30 mK, SdH measurements in it have shown the presence of oscillatory resistivity with the same frequency observed for M samples, albeit with strongly suppressed amplitude (see the supplementary material[18]). Values of lower (ν_1) and higher (ν_2) dHvA frequencies for all graphite are listed in Table I. The frequency observed for S samples coincides with the highest frequency observed for M samples, indicating that this carrier group has the same concentration in every graphite measured.[19] The absence of lower frequency oscillations (ν_1) in S samples can be justified by the overall low amplitude of the dHvA effect in this sample group, not allowing one of the oscillating components of the magnetization to be experimentally resolved.

The suppression of the dHvA oscillations in the S samples can be attributed to a reduced electronic mobility on them. This is confirmed by low-field magnetoresistance (MR) measurements. All samples presented a MR of the type

$$MR \equiv \frac{R(B)}{R(B=0)} - 1 = \mu^2 B^2, \tag{2}$$

which is the B-dependency expected from the Drude theory for a perfectly compensated semimetal. The mobility μ above corresponds to the averaged electronic mobility of electrons (e) and holes (h) ($\mu = \sqrt{\mu_h \mu_e}$). Samples with stronger quantum oscillations presented higher values of μ, as illustrated in Fig. 4. The sample GW, which had stronger quantum oscillations among all graphite (see Fig. 7), presented a value of $\mu = 1.17 \times 10^6 \mathrm{cm^2 V^{-1} s^{-1}}$. This value is two orders of magnitude higher than what was estimated for

TABLE I. Summary of diffractogram, dHvA, and electronic mobility results.

	GW	ZYB	Natural	Kish	SPI-I	SPI-II	SPI-III
FWHM (deg)	0.39	0.76	2.05	4.47	0.89	2.42	3.07
Rocking curve peaks	Multiple	Multiple	Multiple	Multiple	Single	Single	Single
Frequency ν_1 (T)[a]	4.1(1)	4.8(3)	4.4(1)	4.3(1)	N/A[b]	N/A[b]	N/A[b]
Frequency ν_2 (T)[a]	5.6(1)	6.5(3)	6.1(3)	5.8(1)	5.9(1)	N/A[b]	5.9(1)
Estimated μ ($\mathrm{cm^2 V^{-1} s^{-1}}$)	$1.17(5) \times 10^6$	$5.88(4) \times 10^5$	N/M[b]	$1.6(4) \times 10^5$	$5.80(6) \times 10^4$	$1.36(5) \times 10^4$	$6.39(5) \times 10^4$

[a]Extracted from torque measurements at T = 30 mK.
[b]Not applicable (N/A)/Not measured (N/M).

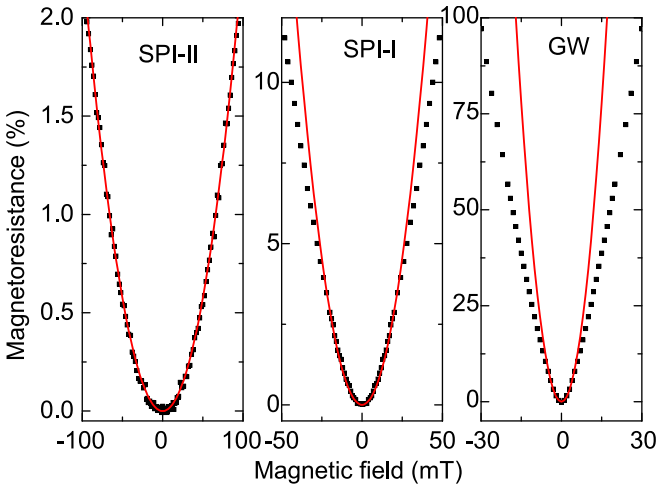

FIG. 4. Magnetoresistance measurements at T = 2 K for different graphite. The points correspond to the experimental data and the lines to a fit of the low field limit by MR = μ^2B^2, with $\mu = 1.36\,\mathrm{T}^{-1}$ for SPI-II, $5.8\,\mathrm{T}^{-1}$ for SPI-I, and $117\,\mathrm{T}^{-1}$ for GW.

SPI-II ($\mu = 1.36 \times 10^4 \mathrm{cm}^2\mathrm{V}^{-1}\mathrm{s}^{-1}$), which did not show any dHvA oscillations down to 30 mK (see Fig. 3). Values of μ for all samples are presented in Table I. Values in brackets correspond to the uncertainty in the least significant digit of data.

The fact that the quantum oscillations are more suppressed in samples with lower electronic mobility is not surprising. However, the question remains on the structural disorder parameters responsible for such suppression, since one cannot correlate values of μ with the FWHM measured for each sample. To clarify this point, we proceed to examine the topography of our samples. The topographies were measured by in-air Atomic Force Microscopy (AFM). High-resolution conical tips were used in contact mode.[20]

Figure 5 shows the AFM images of the GW, Kish, SPI-II, and SPI-III samples. Samples M and S have shown

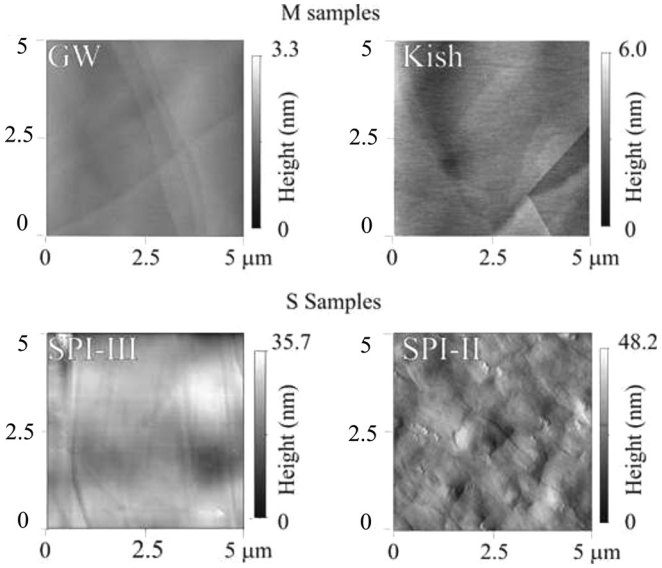

FIG. 5. AFM topographies for four of our samples. Note the different height scales on the right of the figures. Samples belonging to the S group (below) show a much more corrugated surface than samples from the M group (above).

similar results within their groups. The images were obtained from a freshly exposed surface and their main features did not depend on the sampled area or subsequent exfoliations. We see that SPI-II and SPI-III (lower panels) have similar large-scale corrugations on their surface, associated with larger height variations (see the scales in Fig. 5). From the figure, one also notices that the in-plane length of such corrugations in S samples is about 10–100 times smaller than for M samples. For example, the average lateral size of corrugations in SPI-II is approximately 100 nm, while for the GW sample this value is 2–3 μm.

These lateral corrugation sizes are comparable with the mean free paths l^* of charge carriers in our samples, estimated from magnetotransport measurements ($\mu = el^*/(v_f m^*)$). Assuming the effective mass of charge carriers in graphite $m^* \approx 0.05 m_e$ and considering the Fermi velocity $v_F \approx 10^6$ m/s,[21] we obtain $l^* \approx 10$ μm for GW and $l^* \approx 100$ nm for SPI-II, which are similar to the lateral sizes of corrugations (see Fig. 5) and within values reported for HOPG ($0.1\,\mu\mathrm{m} < l^* < 10\,\mu\mathrm{m}$).[22–24] This suggests that the corrugations observed in the AFM measurements are the main source of electronic scattering in the material, limiting the electronic mobility of our samples and suppressing the quantum oscillations measured.

In order to quantify the impact of corrugations on the dHvA oscillations in graphite, we analyzed the rms roughness ($W(l)$) of our samples

$$W(l) \equiv [\langle (h(\vec{r}) - \langle h_l(\vec{r}) \rangle)^2 \rangle_{\vec{r}}]^{1/2}, \tag{3}$$

where $l = |\vec{r} - \vec{r'}|$, $\vec{r'}$ being the origin of the system and $\vec{r}$ an arbitrary position. $W(l)$ is a measure of the contribution to the surface roughness due to fluctuations over a characteristic length scale l.[25] For large values of l, $W(l)$ is expected to converge or oscillate around a finite value corresponding to the average surface's rms roughness.[26] For low values of l, it can be described as $W(l) \propto l^{\alpha}$, where α is defined as the surface roughness exponent.[25,26]

Figure 6 shows the rms roughness calculated from AFM scans (5×5 μm) for all graphite. Samples with corrugated morphology are associated with larger macroscopic roughness exponents (the slopes in Figure 6, $\alpha \approx 0.80$). Values of α in the range of 0.9–1.0 are expected for morphologies presenting pyramid-like features.[26] In our samples, α values for SPI-II (0.82) and SPI-III (0.73) suggest a surface where periodic structures appear but are not so clearly defined. Smaller

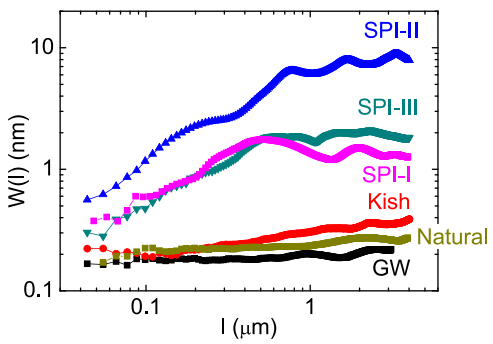

FIG. 6. $W(l)$ for six of our samples. GW has the lowest roughness at all length scales, while SPI-II has the highest.

values of α are observed for the M group, $\alpha \approx 0.05$ and 0.18 (GW and Kish). Such values correspond to experimental observations of smoother macroscopic surfaces.[27]

Figure 7 shows the dHvA oscillations amplitude ΔM of different graphite as a function of their roughness exponents α. In the same figure, the samples' electronic mobilities μ are shown. The data clearly correlate the absence (or strong suppression) of quantum oscillations in graphite with its increased surface roughness. The dependence is roughly of the type $\Delta M \propto \exp(-\alpha \times \text{cte})$, which is the same functional form expected for the suppression of dHvA oscillations with the increase of sample structural disorder (see Eq. (1)).[3,6] Based on these results and in our magnetotransport measurements, we conclude that the presence of wrinkles (or periodic potentials) in graphite limits the mean free path of charge carriers by being the main source of electron scattering, thus suppressing the amplitude of the quantum oscillations observed.

Our results can be further analyzed in light of a theoretical model proposed by Katsnelson and Geim,[28] which predicts that, for weak rippling in graphene ($\alpha < 0.5$), irregularities with radius R and height z affect the sample electronic mobility according to $\mu \propto R^2/z^4$. Considering $R_{GW} \approx R_{Kish}$ and $z_{Kish} \approx 2z_{GW}$ (see Fig. 5), we obtain an expected ratio between GW and Kish mobilities $(\mu_{GW}/\mu_{Kish})_{calc} \approx 15$. The experimental ratio (considering the measured values of μ) is in the range $6 < (\mu_{GW}/\mu_{Kish})_{exp} < 10$ (see Table I). The experimental ratio agrees well with the theoretical modeling, indicating that the main source of electronic scattering in our samples with $\alpha < 0.5$ is indeed the corrugation observed in AFM measurements. Also according to the model, the electronic mobility in samples with $\alpha > 0.5$ should follow $\mu \propto n^{(2\alpha-2)}$, with n the two-dimensional charge carrier concentration (which is assumed to be constant in different samples based on our measured dHvA frequencies). In our SPI-samples, however, the electronic mobility μ decreases with the increase of α (see Fig. 7). This can be understood within the context of rippling if one assumes that the corrugations occurring in the S-samples are strong enough to produce resonant states, in which case the model developed by Katsnelson (for *weak* rippling) is no longer applicable.[28]

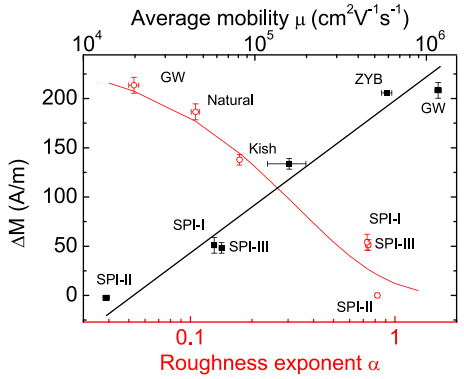

FIG. 7. dHvA oscillation amplitude ΔM as a function of roughness exponent α (open symbols, lower axis) and estimated average mobility μ (closed squares, upper axis) for different samples. The values of ΔM were extracted from SQUID measurements at T = 2 K and B = 2.7 T after the subtraction of a polynomial background from the M(B) curves. The black line is a guide to the eye. The red line is a function of the type $\Delta M = 0.09 \times \exp(-3\alpha)$.

The reduction of electronic mobility with the increase of surface roughness in our samples is qualitatively similar to results in wrinkled graphene sheets. In them, the inclusion of micrometer-long folds in the sample leads to an increase of the electrical resistivity by a factor of 5–10 and a reduction of the electronic mobility up to two orders of magnitude.[28–30] Our results can also be compared to observations in high-mobility two dimensional electron gases in semiconducting heterostructures.[31,32] In these systems, surface roughness is one of the key parameters limiting the electronic mobility. Results in Si MOSFETS and multilayered quantum wells show that the increase of roughness in these structures increases the scattering rate of the electron gas, prompting a reduction of the amplitude of the quantum oscillations.[31–34] For example, the reduction of the width of irregularities in GaAs-GaAlAs quantum wells by a factor of 3 results in a 20-times increase of the quantum oscillations amplitude in the system.[31]

In conclusion, we have shown that sample roughness plays an important role in the suppression of quantum oscillations in graphite. This type of disorder, though important, is not explored in most experiments concerning HOPG. It was observed solely in AFM measurements, being concealed in x-ray diffractometry and Raman spectroscopy. Our experiments have shown that this kind of defect does not affect the FWHM of the x-ray diffractometry rocking-curves but drastically reduces the mobility of the material and is an important disorder parameter that has hitherto been neglected.

We would like to thank Professor Dr. Pablo Esquinazi and Professor Dr. Walter Escoffier for stimulating discussions. This work was carried out with the support of CNPq (Conselho Nacional de Desenvolvimento Científico e Tecnológico—Brasil) and FAPESP (Fundação de Amparo a Pesquisa do Estado de São Paulo).

[1]S. Y. Zhou, G.-H. Gweon, J. Graf, A. V. Fedorov, C. D. Spataru, R. D. Diehl, Y. Kopelevich, D.-H. Lee, S. G. Louie, and A. Lanzara, Nat. Phys. **2**, 595 (2006).
[2]I. A. Luk'yanchuk, Y. Kopelevich, and M. E. Marssi, Physica B **404**, 404 (2009).
[3]I. A. Luk'yanchuk and Y. Kopelevich, Phys. Rev. Lett. **97**, 256801 (2006).
[4]P. Esquinazi, A. Setzer, R. Höhne, C. Semmelhack, Y. Kopelevich, D. Spemann, T. Butz, B. Kohlstrunk, and M. Lösche, Phys. Rev. B **66**, 024429 (2002).
[5]Y. Kopelevich, J. H. S. Torres, R. R. da Silva, F. Mrowka, H. Kempa, and P. Esquinazi, Phys. Rev. Lett. **90**, 156402 (2003).
[6]R. B. Dingle, Proc. R. Soc. London, Ser. A **211**, 517 (1952).
[7]W. Walukiewicz, H. E. Ruda, J. Lagowski, and H. C. Gatos, Phys. Rev. B **30**, 4571 (1984).
[8]G. Hadjisavvas, L. Tsetseris, and S. Pantelides, IEEE Electron Device Lett. **28**, 1018 (2007).
[9]Y. Kopelevich, R. R. da Silva, B. C. Camargo, and A. S. Alexandrov, J. Phys.: Condens. Matter **25**, 466004 (2013).
[10]SPI Supplies, West Chester, PA, USA.
[11]T. L. Makarova, A. L. Shelankov, I. T. Serenkov, and V. I. Sakharov, Phys. Status Solidi B **247**, 2988 (2010).
[12]J. Cervenka, M. I. Katsnelson, and C. F. J. Flipse, Nat. Phys. **5**, 840 (2009).
[13]L. G. Cancado, K. Takai, T. Enoki, M. Endo, Y. A. Kim, H. Mizusaki, A. Jorio, L. N. Coelho, R. Magalhaes-Paniago, and M. A. Pimenta, Appl. Phys. Lett. **88**, 163106 (2006).
[14]J. Barzola-Quiquia, J.-L. Yao, P. Rodiger, K. Schindler, and P. Esquinazi, Phys. Status Solidi A **205**, 2924 (2008).
[15]Kish graphite was originally a by-product of steel manufacture, and it resembles natural graphite.

[16]Quantum Design, Inc., San Diego, CA, USA, see http://www.qdusa.com/.
[17]A. J. Matthews, A. Usher, and C. D. H. Williams, Rev. Sci. Instrum. **75**, 2672 (2004).
[18]See supplementary material at http://dx.doi.org/10.1063/1.4940233 for the SdH measurements and the Fourier analysis of the quantum oscillations shown.
[19]N. W. Ashcroft and N. D. Mermin, *Solid State Physics* (Brooks Cole, 1976), Chap. 2 and 14.
[20]N. Jalili and K. Laxminarayana, Mechatronics **14**, 907 (2004).
[21]D. E. Soule, J. W. McClure, and L. B. Smith, Phys. Rev. **134**, A453 (1964).
[22]G. H. Kinchin, Proc. R. Soc. London, Ser. A **217**, 9 (1953).
[23]Y. Hishiyama, A. Yoshida, and Y. Kaburagi, Carbon **52**, 622 (2013).
[24]N. Garcia, P. Esquinazi, J. Barzola-Quiquia, B. Ming, and D. Spoddig, Phys. Rev. B **78**, 035413 (2008).
[25]M. E. Fisher, J. Chem. Soc., Faraday Trans. 2 **82**, 1569 (1986).
[26]E. Gogolides, C. Boukouras, G. Kokkoris, O. Brani, A. Tserepi, and V. Constantoudis, Microelectron. Eng. **73–74**, 312 (2004).
[27]J. Krim and J. O. Indekeu, Phys. Rev. E **48**, 1576 (1993).
[28]M. Katsnelson and A. Geim, Philos. Trans. R. Soc. London, Ser. A **366**, 195 (2008).
[29]K. Xu, P. Cao, and J. R. Heath, Nano Lett. **9**, 4446 (2009).
[30]V. M. Pereira, A. H. Castro Neto, H. Y. Liang, and L. Mahadevan, Phys. Rev. Lett. **105**, 156603 (2010).
[31]H. Celik, M. Cankurtaran, A. Bayrakli, E. Tiras, and N. Balkan, Semicond. Sci. Technol. **12**, 389 (1997).
[32]N. Balkan, R. Gupta, M. Cankurtaran, H. Celik, A. Bayrakli, E. Tiras, and M. Arikan, Superlattices Microstruct. **22**, 263 (1997).
[33]Y. Cao and D. Jena, Appl. Phys. Lett. **90**, 182112 (2007).
[34]H. Sakaki, T. Noda, K. Hirakawa, M. Tanaka, and T. Matsusue, Appl. Phys. Lett. **51**, 1934 (1987).